

See discussions, stats, and author profiles for this publication at: <https://www.researchgate.net/publication/7108429>

# Water Molecule Adsorption Properties on the BiVO<sub>4</sub> (100) Surface

ARTICLE *in* THE JOURNAL OF PHYSICAL CHEMISTRY B · JUNE 2006

Impact Factor: 3.3 · DOI: 10.1021/jp0555100 · Source: PubMed

---

CITATIONS

30

---

READS

33

2 AUTHORS, INCLUDING:



Mauro Boero

Institut de Physique et Chimie des Matériaux ...

187 PUBLICATIONS 3,481 CITATIONS

SEE PROFILE

Water Molecule Adsorption Properties on the BiVO<sub>4</sub> (100) SurfaceMitsutake Oshikiri<sup>\*,†</sup> and Mauro Boero<sup>‡</sup>

Nanomaterials Laboratory, National Institute for Materials Science, 3-13 Sakura, Tsukuba, Ibaraki 305-0003, Japan, and Center for Computational Sciences, University of Tsukuba, 1-1-1 Tennodai, Tsukuba, Ibaraki 305-8577, Japan

Received: September 28, 2005; In Final Form: February 28, 2006

The water absorption properties at the surface of BiVO<sub>4</sub> are attracting a great deal of attention because the system is a promising candidate as a photocatalyst operating in the visible light range. This has motivated the present investigation via first principles molecular dynamics, which has revealed that a H<sub>2</sub>O molecule is adsorbed molecularly, instead of dissociatively, at the fivefold Bi site with an adsorption energy of ~0.58 eV/molecule. The band gap of the system shrinks slightly (by ~0.2 eV) upon water adsorption and it is likely that oxygen atoms belonging to the adsorbed water molecules to the Bi sites are oxidized, as inferred by the small Bi–O<sub>water</sub> equilibrium distance (~2.6–2.8 Å) very close to the Bi–O bond in the bulk crystal. In the case of water adsorption at a Bi site, the distance between H<sub>water</sub> and V, which is a reduction site, is larger than in the case of adsorption at a V site, indicating that the proton reduction processes may be suppressed.

## Introduction

A photocatalyst able to promote the decomposition of water molecules and operating in the frequency range of visible light (or in a wider wavelength region) is a primary target in solar energy storage technology. To date, the TiO<sub>2</sub>-based photocatalysts have been the most extensively studied; however, despite great efforts,<sup>1</sup> the range of frequencies in which they work is mostly limited to the ultra violet (UV) region. Given this situation, photocatalytic properties of quite a few metal oxides different from TiO<sub>2</sub> have been explored in order to try to overcome this difficulty. As a result, it was found that some vanadates show photocatalytic activities in visible range for water molecule decomposition and, among them, BiVO<sub>4</sub> and InVO<sub>4</sub> represent typical examples. It has already been acknowledged that BiVO<sub>4</sub> can produce only oxygen,<sup>2</sup> whereas, InVO<sub>4</sub> shows hydrogen evolution in the visible range (from UV to 600 nm).<sup>3</sup> Ideally, both H<sub>2</sub> and O<sub>2</sub> evolutions are desirable and in principle it should be possible to obtain them in the visible range and in the near infrared up to wavelengths of about 1 μm (1.2 eV).

In an attempt at investigating these candidate photocatalysts from a microscopic point of view, we present a first principles molecular dynamics study, within the Car–Parrinello scheme (CPMD),<sup>4</sup> of the adsorption properties of H<sub>2</sub>O molecules on the surface of BiVO<sub>4</sub>, using model systems of volume sizes of about 2 nm<sup>3</sup>. We focus on the behavior of water molecule dynamics on the surface of BiVO<sub>4</sub>, equilibrium structures and related electronic structure modifications of the system upon hydration to gain insight into the origin of O<sub>2</sub> generation and the absence of H<sub>2</sub> production in BiVO<sub>4</sub>. We then compare BiVO<sub>4</sub> with the conventional TiO<sub>2</sub> system and with InVO<sub>4</sub>, investigated in our previous work, with respect to their behavior in H<sub>2</sub>O adsorption, aiming at a comprehensive view of the

vanadate catalyst's family. This work might provide some good hints that can be used to pioneer new visible light response photocatalysts able to generate both O<sub>2</sub> and H<sub>2</sub>.

Structural Properties of BiVO<sub>4</sub> Crystal

The BiVO<sub>4</sub> compound has different polymorphs. In our particular case, we selected the distorted sheelite structure (monoclinic) because its photocatalytic activity has been shown to be higher than (at least) a tetragonal BiVO<sub>4</sub>.<sup>2</sup>

We used the crystallographic atomic positions that we had refined via DFT-LDA within the LMTO method by minimizing the total energy in order to match the cell lattice constants,<sup>5</sup> which have been determined accurately through experiments.<sup>3</sup> For simplification, we have approximated the β angle to 90°, which is very close to the reported value from experiments (90.43°).<sup>6</sup> Our theoretical results for *x*, *y*, and *z* parameters are 0.25, 0.13, and 0.10, respectively, with an accuracy of about 0.01. Each atomic position can then be obtained by setting *a* = 5.186 Å, *b* = 5.100 Å, *c* = 11.708 Å, *x* = 0.25, *y* = 0.13, and *z* = 0.10 with the coordinate configuration shown in ref 7. Snapshots of this crystal structure from the [010] and [001] directions, with polyhedra representation, are shown in Figure 1a and b, respectively.

Further detailed geometrical properties can be better understood by comparison with the TiO<sub>2</sub> system as follows. The V site in the BiVO<sub>4</sub> system is surrounded by four oxygen atoms forming a VO<sub>4</sub> tetrahedron (fourfold coordinated V; hereinafter called 4c-V) and the typical V–O distance is 1.86–1.87 Å. Each VO<sub>4</sub> tetrahedron does not make contact with a subsequent VO<sub>4</sub> tetrahedron, and the Bi site is surrounded by eight oxygen atoms located at the corners of eight different VO<sub>4</sub> tetrahedra (Figure 1c), with Bi–O distances of 2.3–2.6 Å (eightfold coordinated Bi; hereinafter called 8c-Bi). Alternatively, the distance of Ti–O in the TiO<sub>6</sub> octahedron in the rutile or anatase crystal phase is about 1.9–2.0 Å.<sup>8</sup>

The V–V distances in BiVO<sub>4</sub> are 3.9 Å, and the shortest O–O distance is 2.6 Å. The Bi atoms are ideally connected by segments of about 3.9 Å to form a continuous zigzag line along

\* To whom correspondence should be addressed. E-mail: oshikiri.mitsutake@nims.go.jp. Phone: +81-29-863-5414. Fax: +81-29-863-5599.

<sup>†</sup> Nanomaterials Laboratory, National Institute for Materials Science.

<sup>‡</sup> Center for Computational Sciences, University of Tsukuba.

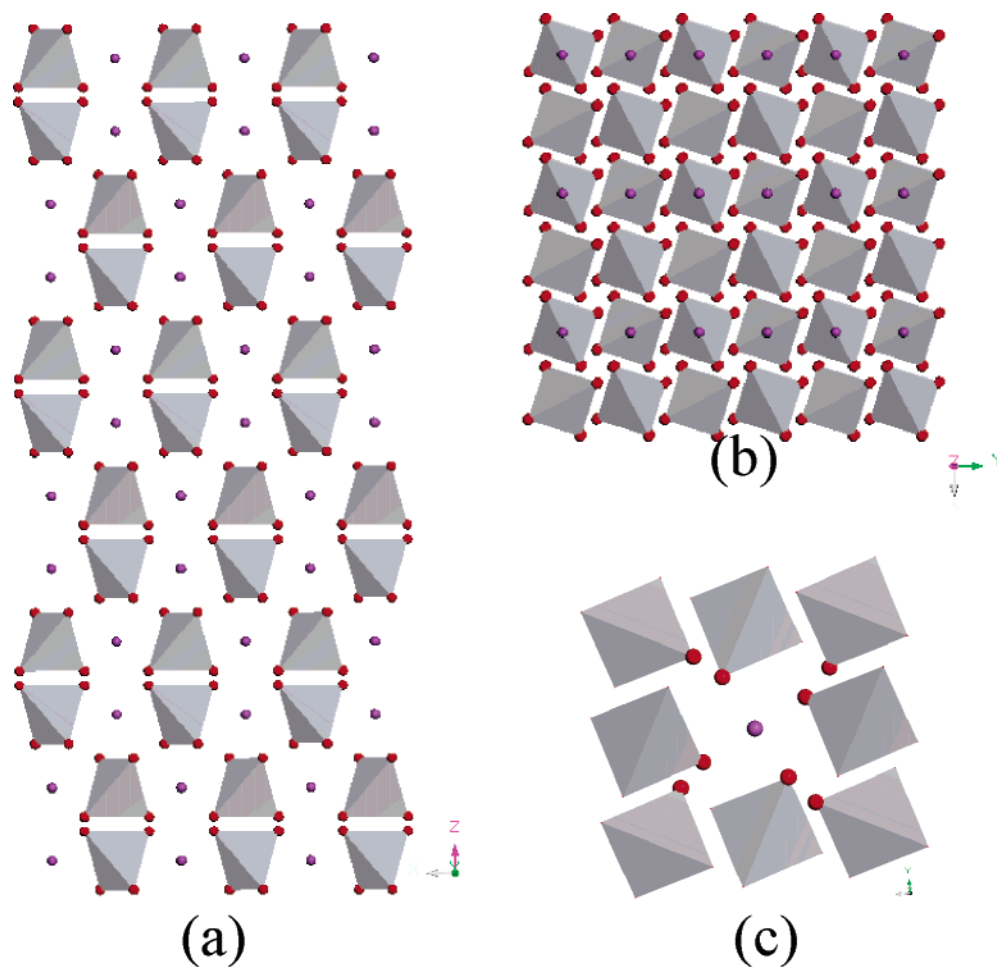


**Figure 1.** Crystal structure of monoclinic BiVO<sub>4</sub>. (a) View from the [010] direction. O and Bi atoms are indicated in red and purple, respectively. V atoms form a tetrahedral, shown in gray, with one O atom at each vertex. (b) View from [001] direction. (c) Bi atoms are surrounded by eight oxygen atoms belonging to eight different VO<sub>4</sub> tetrahedra.

the (100) or (010) plane. The Bi–V distance is approximately 3.6–3.9 Å. The electronic structure of bulk BiVO<sub>4</sub> can be summarized as a conduction band bottom spanned mainly by a V\_3d atomic orbital (~79%) and a valence band top composed of O\_2p (~64%) and Bi\_6s (~18%).<sup>3</sup> A remarkable feature is the large contribution of Bi\_6s components at the top of the valence band. The presence of Bi atoms could compensate, to some extent, for the disadvantage in achieving high hole mobility due to the relatively large O–O separation (2.53 Å (rutile) and 2.45 Å (anatase) in TiO<sub>2</sub>), which would promote the oxidization process. However, the V–V distances of BiVO<sub>4</sub> (3.9 Å) are considerably larger when compared with the Ti–Ti separation in the TiO<sub>2</sub> rutile (2.96 Å) and anatase (3.04 Å).<sup>8</sup> Because the conduction bands of TiO<sub>2</sub> and BiVO<sub>4</sub> are composed mainly of 3d states of Ti and V, the electron conductivity of the BiVO<sub>4</sub> system could be expected to be lower. However, because of the smaller conduction bandwidth resulting from the isolated V atoms, the location of the energy in the conduction band bottom would not be so different from that of TiO<sub>2</sub>. From a close look at the bulk crystal electronic structures of TiO<sub>2</sub> and BiVO<sub>4</sub> as presented in ref 3, it does not seem surprising that BiVO<sub>4</sub> could promote the production H<sub>2</sub>. As a matter of fact, because of the electronic structure of BiVO<sub>4</sub>, V is expected to be a reduction site, whereas the oxidation could occur at either a Bi or an O site; however, by considering the negative results of the experiments, it might be also possible that water molecule adsorption or H<sup>+</sup> access near the V site, which should be a

reduction site because of the electronic structure properties of BiVO<sub>4</sub>, might be suppressed by reasons that remain still unclear.

### Computational Details

First principles dynamical simulations were performed within a Becke–Lee–Yang–Parr (BLYP) gradient corrected approach.<sup>9</sup> The valence-core interaction was described by norm-conserving Troullier–Martins (TM) pseudopotentials for V, Bi, and O atoms, whereas for H we used a Car–von Barth pseudopotential.<sup>10</sup> In the case of V the use of semicore states turned out to be necessary for a good description of both the geometry and the energetics. For Bi, nonlinear core corrections were included. The performance of the Bi pseudopotential was checked carefully by comparison with the experimental lattice constants of  $\alpha$ -Bi<sub>2</sub>O<sub>3</sub>,<sup>11</sup> leading to an error lower than 2%. Other pseudopotentials were checked in a previous work.<sup>3</sup>

The electrons of Bi 5d, 6s, 6p; V 3s, 3p, 3d, 4s; O 2s, 2p; H 1s were included in the valence electrons. Valence wave functions were expanded in plane waves with an energy cutoff of 80 Ry. The surface was represented by a slab, whose bottom layers were kept fixed to the bulk crystal, while the rest of the structure was fully relaxed. The large *z* dimension ensures an empty space (>10 Å), above the relaxed surface, sufficient to keep the system far from its repeated images, because periodic boundary conditions are imposed. The simulated system consists of two unit cells of BiVO<sub>4</sub> corresponding to a global size of *a* × 2*b* × *c*. The super cell size is (*a* + empty space) × 2*b* × *c*

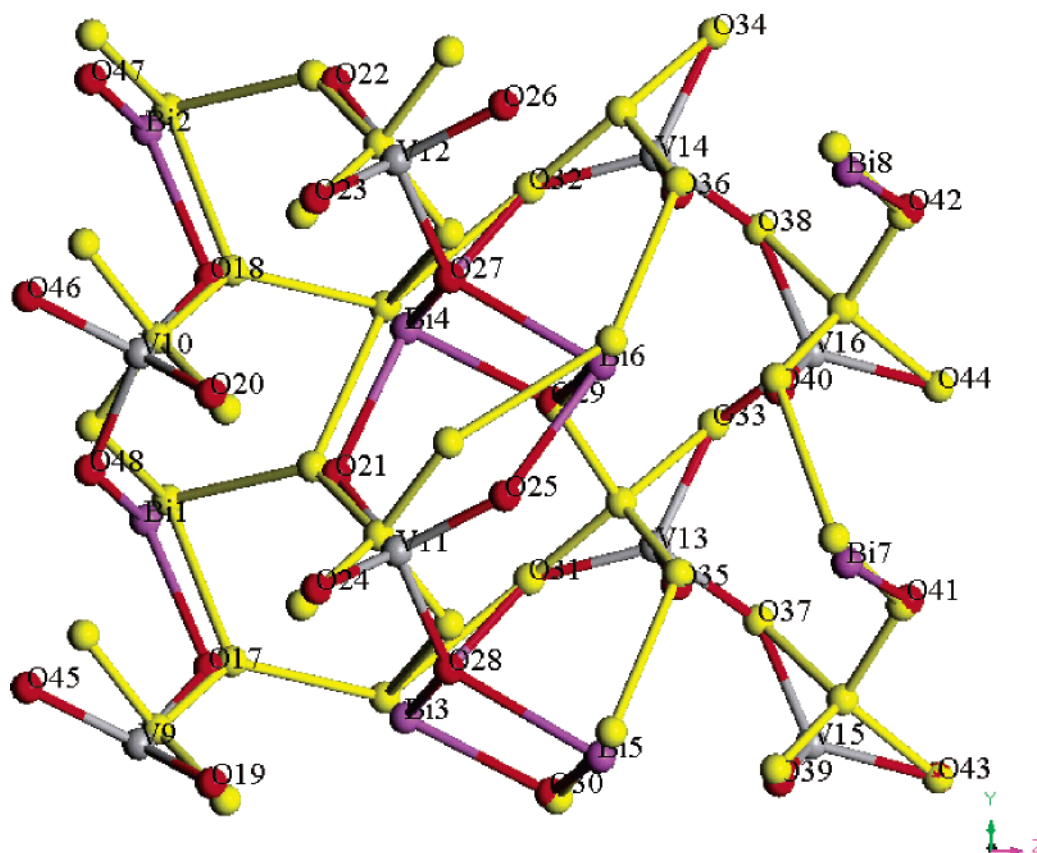


**Figure 2.** Snapshot of the structure relaxation of  $\text{BiVO}_4$  surface. Yellow sticks and balls indicate the bulk crystal structure named B in the text. The relaxed Bi, V, and O atoms are shown in purple, gray, and red balls, respectively, and indicate the structure labeled A in the text, superposed on B. The view shown here is from the  $[100]$  direction.

$= 18.5 \text{ \AA} \times 11.7 \text{ \AA} \times 10.2 \text{ \AA}$  ( $2.2 \text{ nm}^3$ ) and the simulated surface size is  $2b \times c = 11.7 \text{ \AA} \times 10.2 \text{ \AA} = 119 \text{ \AA}^2$ . A fictitious electronic mass of 1200 au and an integration step of 5.0 au ensured good control of the conserved quantities.

We focused on the (100) surface, where the O and Bi atoms are exposed, both in the absence and in the presence of (one or more)  $\text{H}_2\text{O}$  molecules. The exposed Bi site is surrounded by five oxygen atoms (fivefold coordinated Bi; hereinafter 5c-Bi), and the V site that is closer to the surface is surrounded by four oxygen atoms (4c-V). Because a single  $\text{H}_2\text{O}$  molecule occupies a volume of  $3.1 \times 3.1 \times 3.1 \text{ \AA}^3$  in standard conditions ( $P = 1 \text{ atm}$ ,  $T = 273 \text{ K}$ ), on average, the size of one monomolecular  $\text{H}_2\text{O}$  layer that is needed to completely cover the simulated surface is equivalent to 12  $\text{H}_2\text{O}$ , which corresponds to an area of about  $12 \times 3.1 \times 3.1 = 115 \text{ \AA}^2$ , that is, roughly identical to the surface size of our model. We have confirmed that this surface is indeed stable. However, a surface exposing both V (2c-V) and Bi (4c-Bi) atoms, with 12  $\text{H}_2\text{O}$  molecules on top ready to react, would be much more active. Unfortunately such a surface is unstable at 300 K and thus represents an unrealistic system. Eight Bi, 8 V, and 32 O atoms (plus 1  $\text{H}_2\text{O}$ , 2  $\text{H}_2\text{O}$ , or 12  $\text{H}_2\text{O}$ ) are included in the simulation cell and the system is stoichiometric with a neutral global charge. Throughout all calculations, eight oxygen atoms belonging to the bottom layer are fixed to the bulk crystal coordinates and all geometry optimizations (GO) were carried out until the residual forces were less than 0.0002 Hartree/au unless otherwise specified.

The energy of the water molecule absorption was estimated by placing a single or double  $\text{H}_2\text{O}$  molecule on the surface in order to exclude the energy contributions coming from complicated hydrogen bonding occurring at the stage of water cluster formation and, on a second instance, to investigate the adsorption

energy dependence on the coordination number of oxygen atoms around Bi sites. Because adsorption of only one  $\text{H}_2\text{O}$  molecule, which forms 6c-Bi, might result in overestimating the stability of the species with the lower coordination number, in this study, we checked the adsorption energy in the case of seven-coordinated Bi (7c-Bi).

The substrate relaxation energy was estimated by first computing the total energy of the system ( $E_s$ ) in the absence of water molecules via GO after applying constant temperature molecular dynamics (CPMD) to equilibrate the system. The total energy of the water molecule ( $E_w$ ) was then calculated by simple GO. If the total energy of the fully relaxed system with one water molecule after GO is defined as  $E_{\text{all}}$ , then the absorption energy  $E_{\text{abs}}$  of one water molecule is  $E_{\text{abs}} = (E_s + E_w) - E_{\text{all}}$ .

## Results

As a first step, to check the stability of the cleaved surface and its relaxation in the absence of water, we did a temperature-controlled CPMD at 300 K for about 2.5 ps and then performed GO. The bulk crystal structure obtained previously by LMTO was used as input to the CPMD code and refined by GO after a dynamical run at 300 K for about 1.3 ps using  $a \times 2b \times c$  bulk crystal cell.<sup>3</sup> We carefully compared the relaxed surface (slab) structure (A) with the refined bulk crystal structure (B). The A structure is shown, superimposed to B, in Figure 2. The average displacement from B to A of all of the atoms excluding the eight fixed atoms (O<sub>31</sub>, 32, 33, 34, 37, 38, 43, 44 in Figure 2) is approximately 0.46 Å. The average shifts of the 8 Bi atoms plus the 8 V atoms and the 24 O atoms are 0.44, 0.61, and 0.42 Å, respectively. In particular, the shifts of V<sub>13</sub>, 14, 15, 16

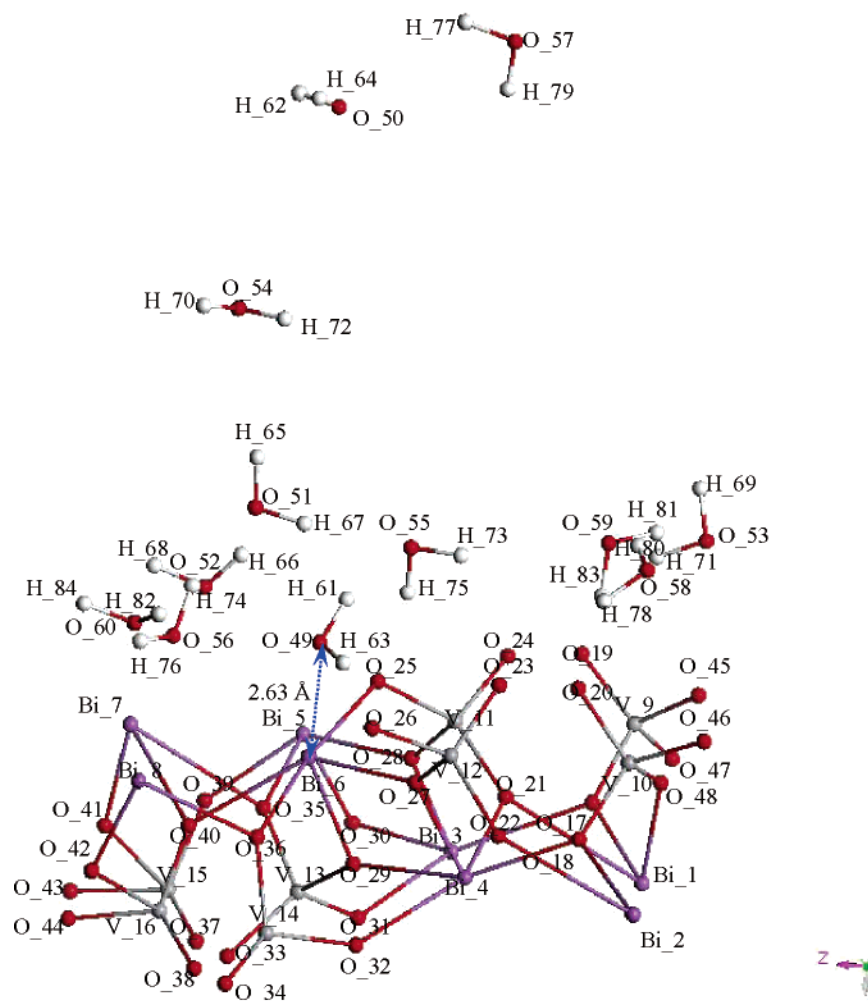


**Figure 3.** Schematic representation from the [010] direction of the geometry of the BiVO<sub>4</sub> slab system with 12 H<sub>2</sub>O molecules on the surface after geometry optimization and 5.1 ps constant temperature dynamics at 300 K. Atomic relaxations were carried out until the residual forces were less than 0.05 Hartree/au. Bi, V, O, and H atoms are indicated by purple, gray, red, and white balls, respectively.

and O<sub>25</sub>, 26, 45, 46 turn out to be relatively large, amounting to 0.87, 0.87, 0.87, and 0.87 Å, and 1.00, 0.99, 1.00, and 0.99 Å, respectively. This indicates that the surface is still stable but subjected to a large modification. We also found that, despite large surface modification, the difference in the band gap obtained by Khon–Sham energy calculation between in A and in B was not very large. Namely, the band gap at the  $\Gamma$  point of B was 2.63 eV and that of A was 2.38 eV. The surface cleavage energy for (100) in our model was roughly estimated to be 0.97 J/m<sup>2</sup>.

In Figure 3, we show the geometry of the system with 12 H<sub>2</sub>O molecules obtained upon GO after 5.1 ps CPMD at 300 K. In this particular case, GO was carried out until the residual forces were lower than 0.05 Hartree/au. Before going into details of the geometry optimizations, we would like to say a few words about the dynamical features of the system during the CPMD at 300 K.

During the dynamics, we noticed that whenever a water molecule comes in proximity of the (100) surface exposing Bi atoms, a strong interaction occurs between Bi and the lone pairs of the O atom of the H<sub>2</sub>O molecule. A few water molecules are always adsorbed on the exposed Bi atoms; however, no spontaneous dissociative adsorption could be found. The minimum and maximum distances between O atoms belonging to water molecules and Bi on the surface during CPMD, after achieving thermal equilibrium (after ~0.6 ps), are summarized

**TABLE 1: Minimum and Maximum Distances between the Oxygen Atom Belonging to Water Molecules and the Bi Atom on the Surface during CPMD at 300 K at Thermal Equilibrium.**

	min (Å)	max (Å)	initial distance (Å)
O <sub>49</sub> –Bi <sub>6</sub>	2.37	3.35	8.33
O <sub>49</sub> –Bi <sub>8</sub>	2.49	5.05	6.16
O <sub>52</sub> –Bi <sub>5</sub>	2.43	4.62	5.07
O <sub>52</sub> –Bi <sub>7</sub>	2.75	5.14	6.07
O <sub>56</sub> –Bi <sub>6</sub>	2.65	5.53	5.60
O <sub>56</sub> –Bi <sub>7</sub>	2.34	3.83	4.67
O <sub>60</sub> –Bi <sub>8</sub>	2.77	5.38	4.92

in Table 1. Although the water molecules including O<sub>49</sub>, 52, 56, 60 sometimes flew away from Bi sites to distances larger than 5 Å, at thermal equilibrium they tend to stay close to Bi atoms at the surface in a stable water adsorption (average) configuration. Furthermore, water molecules are never adsorbed directly at exposed 4c-V sites, but we could see the formation of hydrogen bonds between O atoms coordinated to the V atoms and the H atoms belonging to the water molecules. We have also not observed any formation of H–O–V structure, with H provided by H<sub>2</sub>O to VO<sub>4</sub> tetrahedra. The V atoms show a tendency to keep no more than four O atoms in their coordination shell without exchanging O atoms with H<sub>2</sub>O or allowing O atoms of the water monomers to enter as a member of VO<sub>4</sub>



**TABLE 2: Geometrical Properties When 12 Water Molecules Are Simultaneously Present on the (100) BiVO<sub>4</sub> Surface after Static Geometry Optimization and 5.1 ps Temperature-Controlled CPMD at 300 K<sup>a</sup>**

atomic distances between atoms in water molecules and atoms in a substrate			
atoms belonging to H <sub>2</sub> O	atoms belonging to the surface	distance (Å)	note
O_49	Bi_6/Bi_8	2.63/4.20	H_61–O_49–H_63
O_52	Bi_7/Bi_5	2.99/3.56	H_66–O_52–H_68
O_56	Bi_7/Bi_6	3.01/3.37	H_74–O_56–H_76
O_60	Bi_8	3.31	H_82–O_60–H_84
H_75/O_55	O_25	1.81/2.77	H_73–O_55–H_75
H_83/O_59	O_20	1.90/2.84	H_81–O_59–H_83
H_76/O_56	O_46	1.98/2.74	
H_78/O_58	O_19	2.30/3.00	H_78–O_58–H_80
H_77/O_57	O_32	2.00/2.83	H_77–O_57–H_79, on the neighbor layer
H_64/O_50	O_33	2.71/3.14	H_62–O_50–H_64, on the neighbor layer
atomic distances between water molecules			
atom belonging to H <sub>2</sub> O	atom belonging to other H <sub>2</sub> O	distance (Å)	note
H_84/O_60	O_58	1.93/2.87	
H_74/O_56	O_51	1.95/2.87	
H_66/O_52	O_51	2.12/2.92	
H_67/O_51	O_55	2.11/3.06	H_65–O_51–H_67
H_68/O_52	O_53	2.23/3.14	H_69–O_53–H_71
H_80/O_58	O_59	2.38/3.24	
H_82/O_60	O_52	2.39/3.33	
water molecules, H_70–O_54–H_72 are almost free.			

<sup>a</sup> Atomic relaxations were carried out until the residual forces were less than 0.05 Hartree/au.

tetrahedra. The distance between the O of H<sub>2</sub>O and V are most of the (simulation) time larger than 4 Å, and even the minimum observed distance (3.46 Å) is still much larger than the typical V–O bonds (1.86–1.87 Å) in bulk crystal. The electronic structure modifications, due to relaxations and electrostatic interactions with incoming water molecules, have also been analyzed in terms of Kohn–Sham orbitals. We found that the HOMO–LUMO difference (at point  $\Gamma$ ) of BiVO<sub>4</sub> film systems with H<sub>2</sub>O adsorbed on the catalyst surfaces just after 5.1 ps CPMD (C) is similar to the case in which no water molecules are present (A). The gap of A is 2.38 eV and that of C is 2.17 eV, that is, slightly reduced by water adsorption by about 0.2 eV.

Performing GO after the dynamics resulted in four water molecules being adsorbed molecularly at the Bi sites (Bi\_5, 6, 7, 8) on the surface, as shown in Figure 3. The shortest distance is 2.63 Å for Bi\_6–O\_49. This distance is almost the same as the Bi–O distance in the 8c-Bi of the bulk crystal (2.3–2.6 Å). Bi\_5 coordinates one water molecule while Bi\_6, 7, 8 coordinates two water molecules (Table 2). Consequently, these Bi atoms are surrounded by six or seven oxygen atoms. Several water molecules form hydrogen bonds with the exposed O atoms, and some H<sub>2</sub>O molecules form hydrogen bonds among them. Only one water molecule is unbound. The geometric properties are listed in Table 2. The HOMO–LUMO gap (at  $\Gamma$  point) after GO (D) is 2.23 eV. As a further check, after removing the BiVO<sub>4</sub> substrate, we computed the band gap of the cluster formed by just 12 water molecules; the estimated gap turned out to be 3.21 eV, which is much larger than that of D.

To obtain the adsorption energy per single water molecule, we performed GO on the system after removing 10 or 11 of the 12 water molecules from the model described above. In estimating the adsorption energy from the formation of six-coordinated Bi (6c-Bi), we selected the single molecule left on the surface (H\_61–O\_49–H\_63 (Figure. 3)) because it was

characterized by the shortest O<sub>water</sub>–Bi<sub>catalyst</sub> distance and the largest adsorption energy among all of the water molecules composing the monolayer. In general, identification of the maximum adsorption energy for a given surface is helpful in guessing the adsorption *priority* in a mixed gas or liquid that contains several kinds of molecules. On the other hand, to check the water molecule adsorption energy in the seven-coordinated Bi (7c-Bi), the water molecules H\_61–O\_49–H\_63 and H\_74–O\_56–H\_76 in Figure 3 were left on the surface because the H\_74–O\_56–H\_76 was located to a distance corresponding to a second nearest neighbor to the concerned Bi. A full relaxation was then performed until the residual forces were less than 0.0003 Hartree/au. Figure 4a shows the geometry of this single H<sub>2</sub>O adsorption on the (100) BiVO<sub>4</sub> surface, adsorbed in a nondissociated form. The bismuth atom labeled Bi\_6 at the surface is surrounded by six oxygen atoms, labeled O\_25, 27, 29, 36, 40 (belonging to the catalyst), and O\_49 (belonging to the adsorbed H<sub>2</sub>O molecule). The Bi–O equilibrium distances are 2.23, 2.23, 2.22, 2.54, 2.62, and 2.75 Å, respectively. They are not much different from the typical Bi–O bond of the bulk crystal (2.3–2.6 Å; 2.43 Å on average) where a shell of eight O atoms surrounds Bi. O\_49 undergoes a Coulomb attraction toward Bi\_8 to an equilibrium distance of 3.46 Å. Furthermore, the hydrogen atom labeled H\_51 belonging to the water molecule interacts with the surface O\_26 of BiVO<sub>4</sub>. The equilibrium distance of H\_51 and O\_26 is 1.68 Å, and the separation between O\_49 and O\_26 is 2.65 Å, typical of a hydrogen bond. The geometrical properties are summarized in Table 3. The estimated absorption energy of H<sub>2</sub>O to Bi turns out to be ~0.58 eV per molecule, which includes the energy of the hydrogen bond of O\_49–H\_51···O\_26–V\_17 and takes into account the surface relaxation energy. This value is comparable to the case of TiO<sub>2</sub> anatase.<sup>12</sup> Figure 4b shows the geometry of the double H<sub>2</sub>O molecule adsorption on the (100) BiVO<sub>4</sub> surface, adsorbed in a nondissociated form. The bismuth atom labeled Bi\_6 at the surface is surrounded by seven oxygen

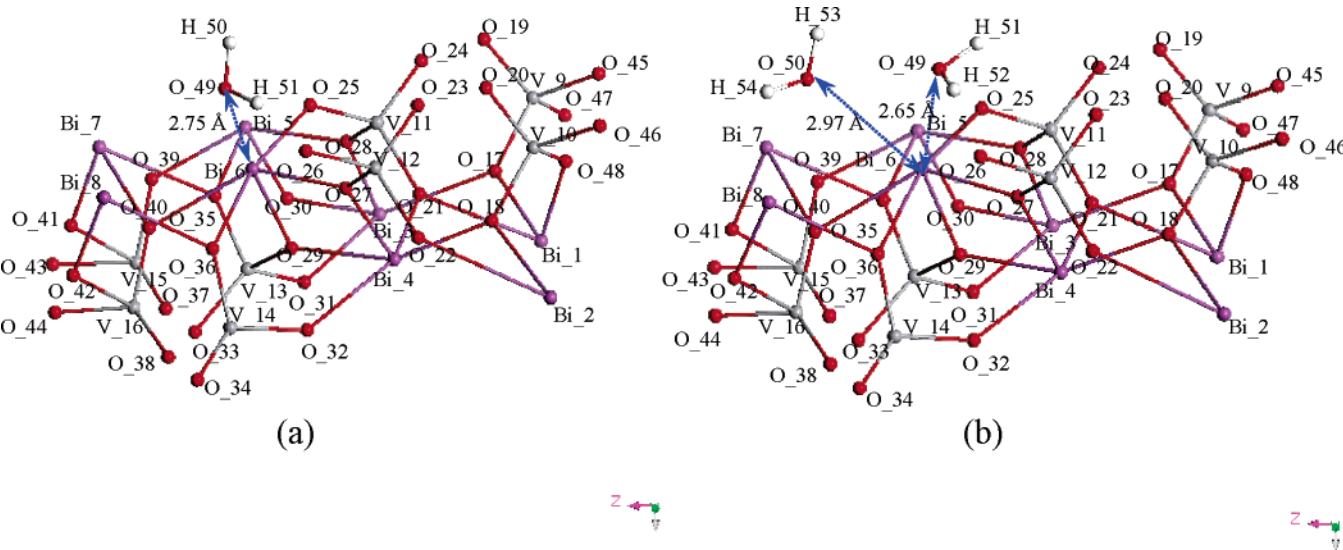


**Figure 4.** View of the geometry of the BiVO<sub>4</sub> slab system from the [010] direction, with (a) a single H<sub>2</sub>O molecule and (b) two H<sub>2</sub>O molecules on the surface, obtained after geometry optimization. Atomic relaxations were carried out until the residual forces were less than 0.0003 Hartree/au. Bi, V, O, and H atoms are indicated by purple, gray, red, and white balls, respectively.

**TABLE 3: Geometric Properties When a Single Water Molecule Is on Top of the (100) BiVO<sub>4</sub> Surface, Obtained via Geometry Optimization with Residual Forces Lower than 0.0002 Hartree/au**

atomic distances between atoms in water molecules and atoms in a substrate			
atoms belonging to H <sub>2</sub> O	atoms belonging to the surface	distance (Å)	note
O_49	Bi_6/Bi_8/Bi_5	2.75/3.46/4.14	H_50–O_49–H_51,
H_50/H_51	Bi_6	3.37/3.11	0.973 Å, 1.01 Å, 106.8°
H_50/H_51	Bi_8	4.23/3.79	Bi_6–O_49–H_51–O_26–V_12,
H_51/O_49	O_26	1.68/2.65	2.75 Å, 1.01 Å, 1.68 Å, 1.73 Å
H_51	Bi_5/V_12	3.41/2.83	
bond angles (deg)			
	Bi_6–O_49–H_50	122.5	
	Bi_6–O_49–H_51	101.4	

**TABLE 4: Geometric Properties When Two Water Molecules Are on Top of the (100) BiVO<sub>4</sub> Surface, as Obtained upon Geometry Optimization (Residual Forces Lower than 0.0003 Hartree/au)**

atomic distances between atoms in water molecules and atoms in a substrate			
atoms belonging to H <sub>2</sub> O	atoms belonging to the surface	distance (Å)	note
O_49	Bi_6/Bi_8	2.65/4.51	
O_50	Bi_6/Bi_7/Bi_8	2.97/2.99/3.74	H_51–O_49–H_52,
H_51/H_52	Bi_6	3.11/3.07	0.976 Å, 0.996 Å, 105.0°
H_53/H_54	Bi_6	3.49/3.55	H_53–O_50–H_54,
H_53/H_54	Bi_7	3.74/3.25	0.972 Å, 1.01 Å, 106.9°
H_53/H_54	Bi_8	4.32/3.10	Bi_6–O_49–H_52–O_26–V_12,
H_52/O_49	O_26	1.81/2.74	2.65 Å, 0.996 Å, 1.81 Å, 1.73 Å
H_54/O_50	O_46	1.70/2.67	Bi_6–O_50–H_54–O_46–V_10,
H_52	Bi_5/V_12	3.81/2.68	2.97 Å, 1.01 Å, 1.70 Å, 1.78 Å
H_54	V_10	2.97	
bond angles (deg)			
	Bi_6–O_49–H_51	109.1	
	Bi_6–O_49–H_52	105.0	
	Bi_6–O_50–H_53	114.3	
	Bi_6–O_50–H_54	117.5	

atoms, labeled O\_25, 27, 29, 36, 40 (belonging to the catalyst), and O\_49, 50 (belonging to the adsorbed H<sub>2</sub>O molecule). The distance of O\_49–O\_50 is 3.23 Å. O\_49 is strongly attracted only to Bi\_6; on the contrary, O\_50 is drawn not only to Bi\_6 but also to Bi\_7. Further details about the local geometric properties of this double H<sub>2</sub>O adsorption are summarized in Table 4. The total adsorption energy of the two water molecules,

including the hydrogen bond energy (O\_49–H\_52···O\_26–V\_12 and O\_50–H\_54···O\_46–V\_10) of the two adsorbed H<sub>2</sub>O molecules, was 1.13 eV. The simple average adsorption energy per water molecule is ~0.56 eV, which is slightly smaller than the corresponding value in the case of single molecule adsorption. Because water molecule adsorptions on the metal oxide catalyst surfaces is accompanied very frequently by such

a kind of hydrogen bonds (for example, O<sub>49</sub>–H<sub>52</sub>···O<sub>26</sub>–V<sub>12</sub> or O<sub>50</sub>–H<sub>54</sub>···O<sub>46</sub>–V<sub>10</sub> in Figure 4b), a single-event adsorption energy to the Bi site might not be very meaningful. What we can infer is that the individual coordination energy per one water molecule to the Bi atom would be on the order of ~0.4 eV if typical hydrogen bond energies are supposed to be 0.1–0.3 eV.

## Discussions

We noticed throughout our simulation that the adsorbed water molecules were stable and that their absorption is nondissociative on the BiVO<sub>4</sub> system, where only Bi atoms are exposed. This might indicate that an activation barrier, larger than the simple thermal oscillations seen during the dynamics, must be overcome in order to obtain H<sub>2</sub>O dissociation. In the well-known TiO<sub>2</sub> system, dissociative adsorption occurs easily even when the activation energy is difficult to determine.<sup>12</sup> We also checked the adsorption properties using a rutile TiO<sub>2</sub> system in which the (001) surface was exposed and the Ti atoms at the surface coordinated four oxygen atoms (4c-Ti).<sup>13</sup> In that system, when a water molecule neared the Ti atoms at distances of about 2.0 Å, the H<sub>2</sub>O molecule dissociates, releasing H<sup>+</sup>. Sometimes the H<sup>+</sup> moves around for a while without forming stable bonds with oxygen atoms at the surface, while at other times, H<sup>+</sup> exchanges are observed between water molecules via dissociative adsorptions. In such situations, we can infer a high probability of H<sup>+</sup> taking an electron from the Ti atoms. On the contrary, in BiVO<sub>4</sub>, H atoms are always bound to nearby O atoms of water, and water molecules are stable because their minimum distance from exposed Bi is still relatively large (2.34 Å, see Table 1.). A behavior similar to that of the TiO<sub>2</sub> system was observed in the InVO<sub>4</sub> system, in which 3c-V atoms were exposed at the surface. When the oxygen atoms of H<sub>2</sub>O molecules approach to within about 2.0 Å of the V atoms at the surface, the water undergoes dissociation.<sup>13</sup> Increasing the H<sup>+</sup> generation rate seems to require a system in which the distances between the cations and oxygen atoms of adsorbed water are short.

In a previous study,<sup>3</sup> we clarified that the valence band of BiVO<sub>4</sub> is composed of not only O<sub>2p</sub> (64% in bulk) but also Bi<sub>6s</sub> (18% in bulk). The conduction band is spanned mainly by V<sub>3d</sub> (79% in bulk), with each V surrounded by four O atoms, forming a tetrahedron. Each VO<sub>4</sub> tetrahedron is separated from the others, with Bi atoms filling the spaces between the VO<sub>4</sub> tetrahedra. Thus, if a hole is created by photoexcitation, then the hole wave function is expected to spread widely in the crystal because of the O<sub>2p</sub> and Bi<sub>6s</sub> orbitals. The hole wave function should then also have nonnegligible amplitudes around the Bi atoms at the surface. According to our findings, an H<sub>2</sub>O molecule adsorbed onto Bi atoms is stable and the distances between the O atoms belonging to H<sub>2</sub>O molecules and the Bi atoms at the surface range between 2.7 and 3.0 Å. This is similar to the Bi–O bond length in bulk. This situation would enhance the oxidization process of H<sub>2</sub>O, that is, extracting electrons from the adsorbed H<sub>2</sub>O. Alternatively, the excited electron would stay close to the V atoms (V 3d-like orbitals) because of the peculiar electronic structure and would be surrounded by the hole wave function resulting from O<sub>2p</sub> and Bi<sub>6s</sub>. Thus, the excited electrons localized in the vicinity of V would not be transferred easily to the H<sup>+</sup> to form H<sub>2</sub>. Most likely, the majority would

recombine, passing from V to O or Bi without generating H<sub>2</sub>. A large recombination rate from V to O or Bi would hamper not only the reduction process but also the oxidation process. O<sub>2</sub> has not been generated from pure water using BiVO<sub>4</sub> catalysts but this system can generate O<sub>2</sub> in the presence of electron acceptors, like Ag<sup>+</sup>, provided by a *sacrificial* reagent, such as AgNO<sub>3</sub>.<sup>2</sup> If the Ag<sup>+</sup> could attract H<sub>2</sub>O to a sufficiently short distance, then it might not only play the role of an electron acceptor but could also enhance the dissociation of H<sub>2</sub>O. This would be an interesting subject for future research.

If V atoms could be exposed on the surface without destabilization, then electrons would transfer to H<sup>+</sup>. Unfortunately, this study found that such a structure tended to be unstable. In the case of InVO<sub>4</sub>, the V and In atoms, which form the conduction band bottom, can be exposed, and the resulting surface is relatively stable.<sup>13</sup> The exposed V atoms have a tendency to capture H<sub>2</sub>O molecules, with the V–O distances less than 2.0 Å, and water molecules often dissociate into –OH<sup>–</sup> and –H<sup>+</sup>. In fact, it has been confirmed in experiments that the InVO<sub>4</sub> system can produce H<sub>2</sub>.<sup>14</sup> We can infer that the manner in which the O atoms coordinate around V at the catalyst surface is a key to obtaining high performance photocatalyst in vanadate systems. To maintain the conduction band bottom of the vanadate system at the appropriate position along the energy axis to promote the reduction of the proton, large V–V separations are also important. Otherwise the width of conduction band spanned mainly by V<sub>3d</sub> would become large, resulting in the failure to reduce the protons because of the lower electron affinity.

Much easier decomposition can be expected when the target molecule is characterized by a size larger than H<sub>2</sub>O so that the O atom belonging to the target reactant is adsorbed at the Bi site and the other part of the molecule is close to the V site. This suggests that BiVO<sub>4</sub> is more suited to decomposing larger molecules. Instead, when water molecules are adsorbed at the Bi sites, the distance between the H and V atoms becomes too large.

## References and Notes

- (1) Asahi, R.; Morikawa, T.; Ohwaki, T.; Aoki, K.; Taga, Y. *Science* **2001**, *293*, 269.
- (2) (a) Kudo, A.; Omori, K.; Kato, H. *J. Am. Chem. Soc.* **1999**, *121*, 11459. (b) Kudo, A.; Ueda, K.; Kato, H.; Mikami, I. *Catal. Lett.* **1998**, *53*, 229.
- (3) Oshikiri, M.; Boero, M.; Ye, J.; Zou, Z.; Kido, G. *J. Chem. Phys.* **2002**, *117*, 7313.
- (4) Car, R.; Parrinello, M. *Phys. Rev. Lett.* **1985**, *55*, 2471.
- (5) (a) Andersen, O. K. *Phys. Rev. B* **1975**, *12*, 3060. (b) Andersen, O. K.; Jepsen, O. *Phys. Rev. Lett.* **1984**, *53*, 2571.
- (6) Bridge, P. J.; Pryce, M. W. *Mineral. Mag.* **1974**, *39*, 847.
- (7) Kay, M. I.; Frazer, B. C.; Almodovar, I. J. *Chem. Phys.* **1964**, *40*, 504.
- (8) (a) Cromer, D. T.; Herrington, K. *J. Am. Ceram. Soc.* **1955**, *77*, 4708. (b) Kim, D.-W.; Enomoto, N.; Nakagawa, Z.; Kawamura, K. *J. Am. Ceram. Soc.* **1996**, *79*, 1095.
- (9) (a) Becke, A. D. *Phys. Rev. A* **1988**, *38*, 3098. (b) Lee, C.; Yang, W.; Parr, R. G. *Phys. Rev. B* **1988**, *37*, 785.
- (10) Troullier, N.; Martins, J. L. *Phys. Rev. B* **1982**, *43*, 1993.
- (11) Harwig, H. A. Z. *Anorg. Allg. Chem.* **1978**, *444*, 151.
- (12) Vittadini, A.; Selloni, A.; Rotzinger, F. P.; Grätzel, M. *Phys. Rev. Lett.* **1998**, *81*, 2954.
- (13) Oshikiri, M.; Boero, M.; Ye, J. *Mater. Res. Soc. Symp. Proc.* **2003**, *751*, Z3.55.
- (14) Ye, J.; Zou, Z.; Oshikiri, M.; Matsusita, A.; Shimoda, M.; Imai, M.; Shishido, T. *Chem. Phys. Lett.* **2002**, *356*, 221.